12th IMEKO TC4 International Symposium
Electrical Measurements and Instrumentation
September 25−27, 2002, Zagreb, Croatia

IMPEDANCE MEASUREMENT USING SINE FITTING ALGORITHMS

Manuel Fonseca da Silva, Pedro Miguel Ramos, António Cruz Serra

IT/ DEEC, IST, Universidade Técnica de Lisboa, Lisbon, Portugal

Abstract − This paper describes an impedance measurement technique based on the use of a personal computer, two digitizing channels and the application of a four parameter sine fitting algorithm, that estimate amplitude, phase, offset and frequency of the voltages across the impedance under measurement and of a reference impedance.

This simple and inexpensive setup leads to experimental results with accuracy comparable to those obtained with sophisticated high cost dedicated impedance measurement equipment. The results here presented, obtained by using a low cost 12 bit PC data acquisition board, for impedances with magnitudes below 1kΩ at 1kHz, show relative standard deviations of $|\bar{Z}|$ below 0.002% and standard deviations for the measured phase under 0.001º.

Keywords: Impedance measurement, sine fitting.

1. INTRODUCTION

A large number of new impedance measurement methods have been presented in the last years [1-6]. Many of them are based on classic measurements methods, modified by using Data Acquisition Boards (DAQs), electronic circuitry and personal computers (PCs) or microprocessors. The inclusion of low cost, but powerful, PCs enables the implementation of sophisticated calibration techniques and digital signal processing algorithms that contribute to significantly reduce the errors of these measurement systems. However, the use in many of them of active devices, such as operational amplifiers, analog multipliers, phase detectors, or modulators, introduces new problems related with their nonideal behavior, especially when the frequency of measurement increases.

The impedance measurement technique the authors described in [1] was based on the classical Schering bridge for capacitance measurement modified by the inclusion of electronic circuitry and a PC. The accuracy of this technique was largely dependent on the performance of the sine fitting algorithms. For that reason, a new algorithm that largely increases the convergence of the traditionally used ones [7] was developed [8,9]. It assures convergence to the minimum of the error function even in cases of acquisition of a small number of samples and/or samples per period, in the presence of noise standard deviation as high as 20% of the rms value of the sine wave and when saturation of the digitizer occurs.

Since one of the main limitations of the former method [1] is originated by the non ideal behavior of operational amplifiers and analog multipliers when the frequency increases, the idea of reducing the measurement circuit to its minimum possible configuration, the impedance under measurement plus a reference impedance, was growing up. This corresponds to the old ammeter, voltmeter technique, Fig.1, now improved by using medium or high resolution Analog-to-Digital Converters (ADCs) and sine fitting techniques. In the present setup the only active devices are those included within the digitizing channels. As far as these channels are accurately characterized at the measurement frequency, by using for instance the histogram method for ADC testing [7,10], a simple look ahead table can be used to implement calibration techniques that will compensate the degradation on the digitizer performance with frequency.

In this paper we will discuss the performance and main limitations of this measurement technique at low frequency and we will show preliminary experimental results.

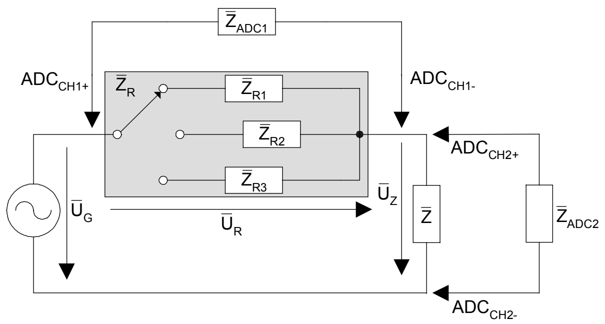

Fig. 1. Measurement circuit.

2. THE MEASUREMENT TECHNIQUE

The measurement procedure is very simple and consists on the following: (i) the generator is adjusted to produce a sinewave with the desired measurement frequency and amplitude; (ii) the digitizing channels simultaneously acquire data records with a large number of samples; (iii) a four parameter sine fitting algorithm is applied in order to obtain the frequencies, amplitudes and phases of the sine waves that best fit the acquired samples; (iv) from the amplitudes and phases of the acquired waveforms the modulus and phase of the impedance under measurement are computed.

The quality of this measurement method depends on the digitizing channels performance, on the accuracy of the knowledge of the reference impedances, on the quality of the calibration techniques and of the sine fitting algorithms.

The systematic errors of the measurement system being time invariant, can be characterized during the calibration process and mathematically removed during the measurement procedure. The identified systematic error sources are, by decreasing order of importance:

1. the inexact knowledge of the reference impedance $\bar{Z}_R$;
2. the inexact knowledge of the input impedance of both digitizing channels ($\bar{Z}_{ADC1}$ and $\bar{Z}_{ADC2}$);
3. the non ideal transfer characteristic of both digitizing channels (this could became the main error source at high frequencies).

All this error sources can be determined during a calibration procedure, with an accuracy that will depend on the quality of the standard impedances used for calibration and the spectral purity of the sinewave generator used to stimulate the digitizing channels during the histogram test [7]. The accuracy of both the calibration and the measurement procedures will increase with the number of bits of the digitizers, but of course that the increase on the number of bits will reduce the system bandwidth.

By its own nature random errors will vary with time in an unpredictable fashion and cannot be removed by calibration. The main random error source is noise inevitably present in any real system, including noise generated within the ADCs. The use of sine fitting techniques can largely reduce the influence of noise in the final results, as shown in Fig.2.

3. SINE FITTING ALGORITHMS

There are many algorithms to perform the least squares curve fits of a sine wave. In [7] two methods are recommended. One estimates three (A , B and C) and the other four (A , B , C and f) parameters of a sine wave, defined as

$$A\cos\left(2\pi f t_m\right)+B\sin\left(2\pi f t_m\right)+C \qquad (1)$$

that fit a set of M samples, $y_1,...,y_M$, acquired at a frequency $f_s = 1/T_s$. The residuals, r_m , of the fit are given by

$$r_m = y_m - A\cos\left(2\pi f t_m\right) - B\cos\left(2\pi f t_m\right) - C\ . \qquad (2)$$

These sine fitting algorithms seek the minimum of

$$\varepsilon_{rms} = \sqrt{\frac{1}{M}\sum_{m=1}^{M} r_m^2}\ , \qquad (3)$$

but must be used with some precautions and the use of records containing at least five cycles is recommended.

If the ratio between signal and sampling frequency is inaccurately known, the four parameter sine fitting algorithm should be used. It seeks solutions of a nonlinear system of equations, which must be solved in an iterative way. From the initial estimated value of the frequency the initial three parameters, A , B and C are computed, the algorithm then produces a new set of values A_i , B_i , C_i and a correction Δf_i to the frequency to be used in the next iteration. The main problem of this algorithm is that the results are highly dependent on the number of samples and especially on the initial estimated values, including naturally the frequency.

In this work the four-parameter sine fitting procedure based on the use of the traditional three parameter sine fitting algorithm performed with an increasing number of acquired samples, in order to avoid convergence to local minimums of the error function, together with a linear regression technique that assures a fast convergence is used [8, 9].

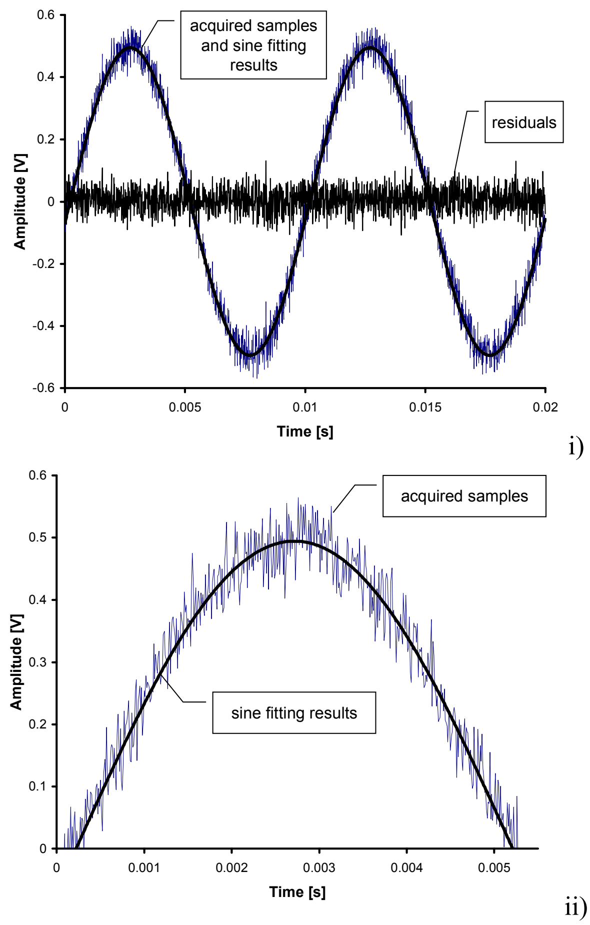

Fig. 2. Sine fitting results in a very noisy environment. In i) the acquired samples and the results of the fitting overlap while the residuals show the added noise. ii) corresponds to a zoom in the section of the first maximum.

4. IMPEDANCE CALCULATION

After the convergence of the two sine fitting procedures (one for channel 1 corresponding to $\bar{U}_R$, and another for channel 2, $\bar{U}_Z$), the final parameters A_x , B_x , C_x and f_x ($x = Z, R$) are obtained. The sine amplitudes are determined through

$$\left|\bar{U}_x\right| = \sqrt{A_x^2 + B_x^2}\ , \qquad (4)$$

while the phase is

$$\phi_{U_x} = \arctan\left(-\frac{B_x}{A_x}\right). \qquad (5)$$

If $A_x < 0$, 180° must be added to ϕ_{U_x}. The values of C_x correspond to small DC components present in the circuit and are disregarded, leading to

$$\bar{U}_x = \left|\bar{U}_x\right| e^{j\phi_{U_x}}\ . \qquad (6)$$

From the circuit of Fig. 1

$$\frac{\bar{U}_\mathrm{R}}{\bar{Z}_\mathrm{Ri} // \bar{Z}_\mathrm{ADC1}} = \frac{\bar{U}_\mathrm{Z}}{\bar{Z} // \bar{Z}_\mathrm{ADC2}}\ .\quad i=1..3 \qquad (7)$$

When, $\bar{Z}_\mathrm{Ri} \ll \bar{Z}_\mathrm{ADC1}$ and $\bar{Z} \ll \bar{Z}_\mathrm{ADC2}$

$$\bar{Z} = \left|\bar{Z}\right| e^{j\varphi} \cong \frac{\bar{U}_\mathrm{Z}}{\bar{U}_\mathrm{R}} \bar{Z}_\mathrm{Ri} = \frac{\left|\bar{U}_\mathrm{Z}\right|}{\left|\bar{U}_\mathrm{R}\right|} \left|\bar{Z}_\mathrm{Ri}\right| e^{j(\phi_{U_\mathrm{Z}} - \phi_{U_\mathrm{R}} + \varphi_\mathrm{R})}\ . \qquad (8)$$

Obviously, the accuracy of this method depends directly on the accuracy of the value of the reference impedance $\bar{Z}_\mathrm{R} = \left|\bar{Z}_\mathrm{R}\right| e^{j\varphi_\mathrm{R}}$.

For each measurement result that will be presented in the next section, a series of N sets of records (each with M points per channel) were acquired. Consequently N values for $\left|\bar{Z}\right|$ and φ were computed. These are used to calculate the average values and the standard deviations of the results for $\left|\bar{Z}\right|$ and φ.

5. RESULTS

The measurement results that will be presented in this section were obtained by using a Keithley DAS1601 data acquisition board with 12 bit resolution and a maximum sampling rate of 50kS/s. The board was used in the range of $\pm 1\mathrm{V}$.

In Fig. 3 the standard deviation of the phase of the impedance under measurement, σ_φ, is plotted against the measured value of the modulus of the same impedance, for almost pure resistive impedances varying from 50Ω to 2kΩ, and using the reference impedance $\bar{Z}_\mathrm{R1}$ shown in Table 1. The two curves correspond to two different ways of choosing the amplitude of $\bar{U}_G$. The first one uses always $\left|\bar{U}_G\right| = 1\mathrm{V}$ regardless of the values of the impedances in the measurement circuit. The second, adapts $\left|\bar{U}_G\right|$ so that the digitizing channel acquiring the signal with the larger amplitude yields $\left|\bar{U}_x\right| \simeq 0.95\mathrm{V}$ (i.e. 95% of the full scale range). This last case requires an additional acquisition to estimate the value of $\left|\bar{U}_G\right|$. However, the results obtained are worth the time and processing required. Obviously this second method reduces the uncertainty of the result by increasing the number of output codes stimulated in both channels and consequently reducing the influence of the quantization error in the final result.

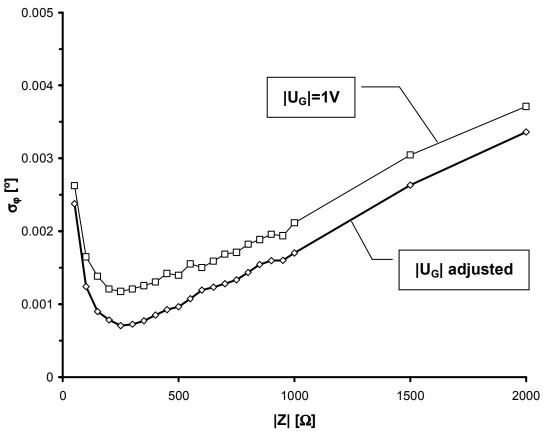

Fig. 3. Standard deviation of the measured phase obtained with a 12 bit digitizer and a sampling rate of 24390S/s. The input frequency is 1kHz and 1000 records of 976 samples corresponding to 40 periods were acquired and processed.

One should expect that the accuracy of this measurement system would depend on the ratio between the reference and the measurement impedance if the same range was used in both channels. In fact, if the moduli of both impedances were not of the same order of magnitude, the amplitude of both voltages would be very different. Even when the generator amplitude is adjusted to grant a maximum excursion of output codes in one channel the other channel will present a very low excursion (and consequently resolution) and will lead to a poor result in the sine fitting algorithm. It is expected that the final prototype to be built should have a few reference impedances, with modulus differing between them by about one order of magnitude in order to assure a large measurement impedance range with high accuracy.

To study the sensitivity of the results to the reference impedance value, three different reference impedances with values shown in Table 1 were used. Fig. 4 shows the standard deviations of φ obtained with these three reference impedances. It can easily be seen that, the final results depend on the sampling impedance value and that the best results are obtained when $\left|\bar{Z}\right| = \left|\bar{Z}_\mathrm{Ri}\right|$.

Table 1. Sampling impedance values measured with the impedance analyzer HP4192A at 1kHz. The uncertainty intervals refer to the maximum error of the measurement according to the instrument specifications.

	$\left\|\bar{Z}_\mathrm{Ri}\right\|$ [Ω]	φ_Ri [°]
$\bar{Z}_\mathrm{R1}$	267.45 ± 0.57	-0.045 ± 0.056
$\bar{Z}_\mathrm{R2}$	332.15 ± 0.71	-0.055 ± 0.056
$\bar{Z}_\mathrm{R3}$	469.25 ± 1.08	-0.045 ± 0.056

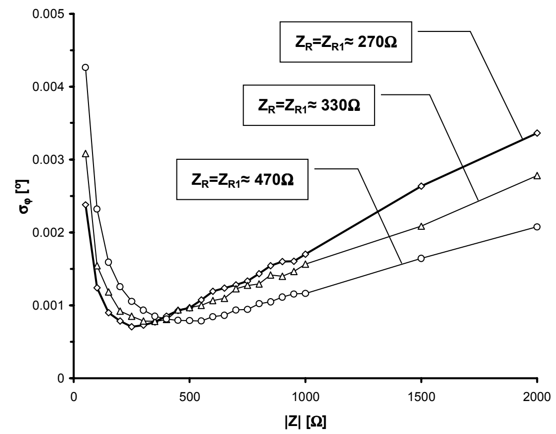

Fig. 4. Same as in Fig. 3 for three sampling impedances and adjusting the generator amplitude to cover 95% of one of the digitizer's channels full-scale range.

To reduce the measurement error, the sampling impedance must be chosen according to the value of the unknown impedance. It can be shown that, the transition values of the intervals ($|Z_{\mathrm{Ti}}|$) where each sampling impedance should be used, in order to minimize the measurement error, are given by

$$|Z_{\mathrm{Ti}}| = \sqrt{|Z_{\mathrm{Ri}}||Z_{\mathrm{Ri+1}}|}\,. \tag{9}$$

For the values of Table 1, the intervals are defined by

$$\bar{Z}_{\mathrm{R}} = \begin{cases} \bar{Z}_{\mathrm{R}1}, & |\bar{Z}| \le 298.0\Omega \\ \bar{Z}_{\mathrm{R}2}, & 298.0\Omega \le |\bar{Z}| \le 394.8\Omega \\ \bar{Z}_{\mathrm{R}3}, & 394.8\Omega \le |\bar{Z}|. \end{cases} \tag{10}$$

In Fig. 5 and Fig. 6 the results obtained by changing the number of acquired periods are shown. The results correspond to the unknown impedance $\bar{Z}_1$. The values of the six unknown impedances under test were measured with the HP4192A and their results as well as the respective uncertainty intervals are presented in Table 2.

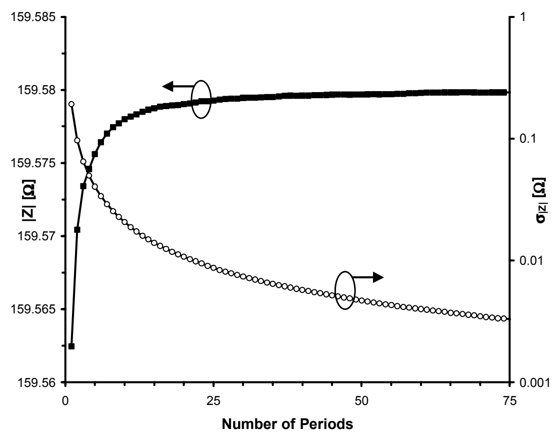

Fig. 5. Average value of the modulus of the impedance and the respective standard deviation. The results correspond to 1000 tests performed at 1kHz with 24390S/s using $\bar{Z}_{\mathrm{R}1}$ as the sampling impedance.

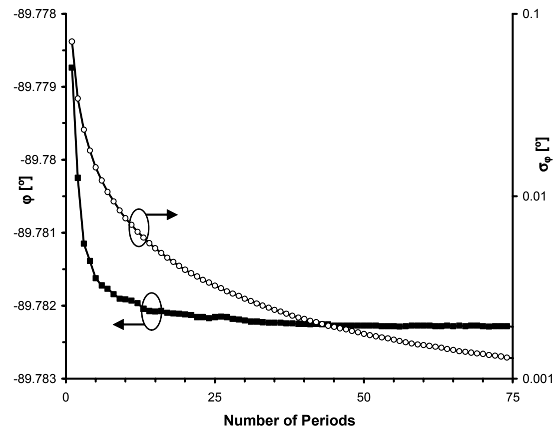

Fig. 6. Same as in Fig. 5 for the phase of the impedance.

It can be seen that, the increase in the number of acquired periods, reduces the standard deviations. This can easily be explained by the error of the results of the sine fitting algorithm. As the number of points increases – corresponding to a higher number of periods, the error of the sine fitting decreases since there are more points of the original data for the algorithm to adjust to. Also, the frequency of the signal is more accurately determined if the number of periods is higher and thus the standard deviation of the phase is reduced.

Table 2. Values of the impedances under measurement obtained with the impedance analyzer HP4192A as in Table 1.

	$\|\bar{Z}_{\mathrm{i}}\|$ [Ω]	φ_{i} [º]
$\bar{Z}_1$	159.5 ± 0.31	-89.775 ± 0.065
$\bar{Z}_2$	278.15 ± 0.59	-53.445 ± 0.061
$\bar{Z}_3$	581.65 ± 1.43	-36.125 ± 0.060
$\bar{Z}_4$	468.75 ± 1.08	-0.045 ± 0.056
$\bar{Z}_5$	342.15 ± 0.74	-89.845 ± 0.065
$\bar{Z}_6$	154.65 ± 0.36	-70.605 ± 0.063

In Fig. 7 the measured average modulus of the impedance and the respective phase together with the corresponding standard deviations as a function of the number of bits of the ADC are shown. The resolution of the ADC is changed by disregarding the less significant bits of the acquired digital words. The interval errors correspond to two times the value of the standard deviations in each case [11].

As can be seen from these results, even for a ADC with 6 bits, the final results are within the uncertainty interval of the HP4192A. As the number of bits increases, the standard deviations are greatly reduced. For this particular impedance, a relative standard deviation $\sigma_{|\bar{Z}|}/|\bar{Z}|$ of 0.00114% was obtained for 12 bits.

In Table 3, the final experimental results obtained for the six impedances under test are presented. These results are all within the specified uncertainty intervals of the HP4192A (Table 2) and present magnitude relative standard deviations below 0.0017% and standard deviations for the phase under 0.001º.

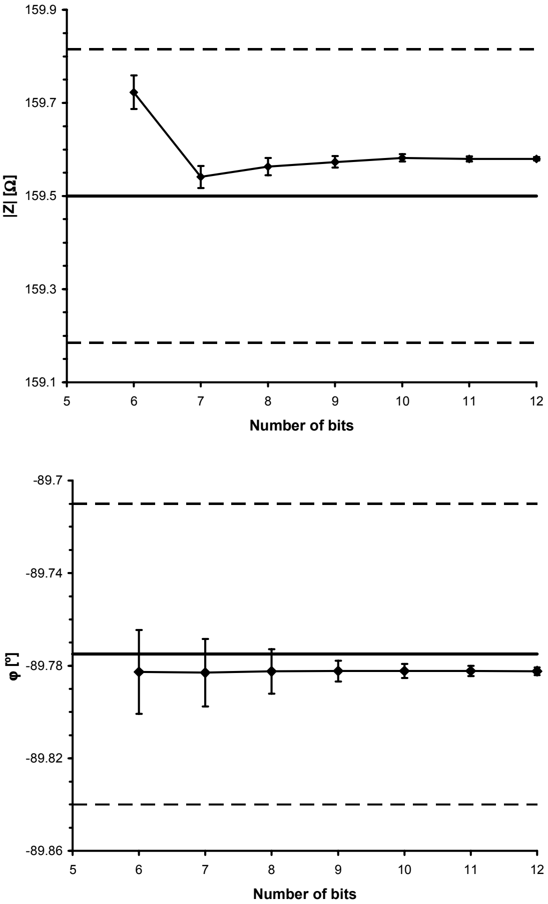

Fig. 7. Measurement results of $\overline{Z}_1$ and respective standard deviations (2σ) as a function of the ADC resolution (164 periods and 24390S/s at 1kHz). The solid thicker lines correspond to the value determined by the HP4192A and the dashed lines represent the interval limits due to the error of the HP4192A.

Table 3. Results obtained for the unknown impedances with 12 bits, 164 periods and 24390S/s at 1kHz.

	$\lvert\overline{Z}_i\rvert$ [Ω]	$\sigma_{\lvert\overline{Z}_i\rvert}$ [Ω]	φ_i [º]	σ_{φ_i} [º]
$\overline{Z}_1$	159.58	1.82m	-89.782	0.820m
$\overline{Z}_2$	278.00	1.83m	-53.462	0.378m
$\overline{Z}_3$	581.38	6.21m	-36.110	0.596m
$\overline{Z}_4$	468.70	4.51m	-0.063	0.327m
$\overline{Z}_5$	342.53	5.80m	-89.765	0.919m
$\overline{Z}_6$	154.76	1.55m	-70.551	0.623m

Since the measured values depend on the accuracy of the sampling impedance, its uncertainty should be reflected in the final results. Although this uncertainty can and will be greatly reduced thru the use of well determined impedances, it can be directly reflected in the final results. The total uncertainty in the phase of the measured impedance is the sum of the measured phase standard deviation with the phase uncertainty of the HP4192A for the measured sampling impedance. The same applies for the modulus of the impedance. These conclusions are a direct result of (8) since we disregarded the effects of the input impedances of the digitizing channels.

In Fig. 8 the real and imaginary parts of $\overline{Z}_1$ are plotted. The circle represents the value indicated by the HP4192A, while the cross is the result obtained with the new technique. The dashed line represents the uncertainty associated with the value measured with the HP4192A, while the solid line depicts the corresponding uncertainty of the present method (two times the standard deviations) – at the scale of this figure, this uncertainty is impossible to distinguish. If the uncertainty on the knowledge of the sampling impedance is taken into account, the final uncertainty interval is the dash-dot line represented in Fig. 8. We again emphasize that this error is not characteristic of the technique but of the uncertainty associated with the sampling impedance – off the shelf resistor measured with the HP4192A. The use of high accuracy (0.01%) resistances commercially available or the use of other more accurate instruments to characterize $\lvert\overline{Z}_{Ri}\rvert$ can drastically reduce this error.

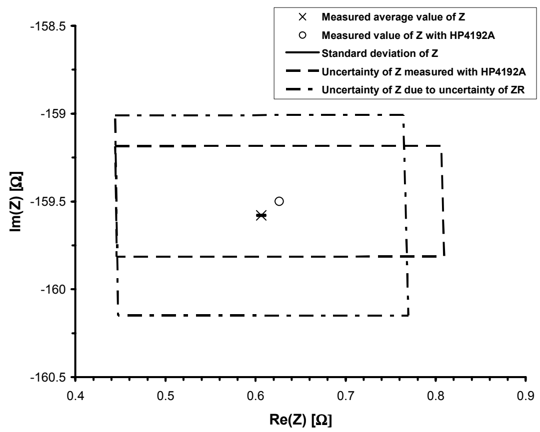

Fig. 8. Experimental results and uncertainty intervals obtained by using the new technique and the HP4192A for $\overline{Z}_1$ in the conditions of the text.

6. CONCLUSIONS

As it can be seen, all the experimental results of this new method are surprisingly good. They compare favorably with the results of high cost dedicated impedance measurement equipment. Results suggest the feasibility of the procedure even with an 8 bit digitizer. If this is confirmed, in the near future every digital oscilloscope could be use to perform high accuracy impedance measurements at high frequencies.

7. ACKNOWLEDGEMENTS

This work was sponsored by the Portuguese national research project entitled “New measurement methods in Analog to Digital Converters testing”, reference PCTI/ESE/32698/1999, whose support the authors gratefully acknowledge.

REFERENCES

[1] M. Fonseca da Silva, A. Cruz Serra, "Study of the sensitivity in an automatic capacitance measurement system", *IEEE Instrumentation and Measurement Technology Conference*, IMTC/97 Proceedings, Vol. 1, pp. 329-334, Ottawa, Canada, May 1997.

[2] W. Yang, "A Self-Balancing Circuit to Measure Capacitance and Loss Conductance for Industrial Transducer Applications", *IEEE Transactions on Instrumentation and Measurement*, IM 45-6, pp. 955-958, Dec. 1996.

[3] K. Mochizuki, K. Watanabe, "A High Resolution Linear Resistance-to-Frequency Converter", *IEEE Transactions on Instrumentation and Measurement*, IM 45-3, pp. 761-764, June 1996.

[4] L. Angrisani, A. Baccigalupi, A. Pietrosanto, "A Digital Signal-Processing Instrument for Impedance Measurement", *IEEE Transactions on Instrumentation and Measurement*, IM 45-6, pp. 930-934, Dec. 1996.

[5] M. A. Atmanand, K. Jagadeesh, V. G. K. Murti, "A Microcontroller Based Scheme for Measurement of L and C", *Measurement Science and Technology*, Vol. 6, pp. 576-581, May 1995.

[6] A. Carullo and A. Vallan, "Impedance Measurement Technique Based on Sine-Fit", *IMEKO 2000*, pp. 249-254, Vienna, Austria, Sept. 2000.

[7] IEEE Std. 1057-1994 *Standard for digitizing waveform records*, New York, Dec. 1994.

[8] M. Fonseca da Silva, A. Cruz Serra, "Improving convergence of sine fitting algorithms", accepted for publication in *Journal of Computer Standards and Interfaces*, Elsevier Science B. V., in press, 2002.

[9] M. Fonseca da Silva, A. Cruz Serra, "A new robust four parameter sine fitting procedure", accepted for presentation in *AADA 2002 and EWADC2002* to be held in Prague, Czech Republic, June 26-28, 2002.

[10] J. Blair, "Histogram Measurement of ADC Nonlinearities", *IEEE Transactions on Instrumentation and Measurement*, vol. 43, pp. 373-383, June 1994.

[11] *Guide to Expression of Uncertainty in Measurement*, First edition 1993, International Organisation for Standardisation 1993.

Authors: Manuel Fonseca da Silva, Pedro Miguel Ramos, António Manuel da Cruz Serra, IT/ DEEC, IST, Universidade Técnica de Lisboa, Av. de Rovisco Pais, 1049-001 Lisboa, Portugal, phone: +351-218418490, fax: +351-218417672, e-mail: fonseca.silva@lx.it.pt, acserra@ist.utl.pt, pedro.ramos@lx.it.pt.